Defect morphology in a biaxial thermotropic polymer

T. De'Neve, M. Kleman, Patrick Navard

Classification
Physics Abstracts
61.30

Defect morphology in a biaxial thermotropic polymer

T. De'Neve ([1]), M. Kleman ([2]) and P. Navard ([3])

([1]) DGA/CREA, 16 bis Avenue Prieur de la Côte d'Or, 94114 Arcueil Cedex, France
([2]) Laboratoire de Physique des Solides, Université de Paris-Sud, Bât. 510, 91405 Orsay Cedex, France
([3]) Ecole Nationale Supérieure des Mines de Paris, Centre de Mise en Forme des Matériaux. Sophia-Antipolis, 06560 Valbonne Cedex, France

(Received 7 August 1991, revised 5 November 1991, accepted 7 November 1991)

Résumé. — Les observations optiques de la texture à fils d'un polymère thermotrope nématique, commercialisé sous la référence VECTRA B950®, ont montré l'existence de trois types de lignes de disinclinaisons, appelées ici E_x, E_y et E_z, de rang demi-entier, parfois associées à des lignes entières. La pluralité de ces défauts est caractéristique de la nature de cette phase nématique biaxe, reliée à des corrélations de rotation interchaînes entre les plans aromatiques. Les relations topologiques entre défauts caractéristiques de la phase biaxe sont vérifiées dans les situations statiques aussi bien que dynamiques. Durant un écoulement de cisaillement, il y a une séparation de E_y en E_x et E_z, à une déformation plus petite que celle correspondant à la multiplication des défauts E_x et E_z.

Abstract. — Optical observations of the thread texture of a nematic thermotropic polymer commercially known as VECTRA B950® have shown the existence of three types of half integer disclination lines, called here E_x, E_y and E_z, sometimes associated with integer disclination lines. This plurality of defects is typical of the biaxial nature of this nematic phase, due to interchain rotational correlations between phenyl rings. The relationships between defects which arise from the topological theory are confirmed, in static as well as in dynamic experiments. During shear flow, there is a splitting of E_y into E_x and E_z at a shear deformation lower than that corresponding to the multiplication of E_x and E_z defects.

1. Introduction.

The existence of a biaxial nematic phase was first predicted by Freiser [1] in 1970 and this phase was indeed discovered by Yu and Saupe [2] in 1980. The academic interest for such a phase has been increasing since then.

The biaxial nematic state is characterised not only by orientational correlations existing between the chain long axes (nematic state) but also by rotational correlations between the two axes describing the aromatic planes (biaxiality). Biaxial phases formed by low molecular weight compounds have been evidenced during the past ten years [3-8].

As far as thermotropic polymers of high molecular weight are concerned, the first study was that of Windle and coworkers [9-13]. The material studied was a copolyester based on 70/30

hydroxynaphtoic acid/hydroxybenzoic acid for which the well-known banded texture was interpreted in terms of phenyl rotation inside the shearing plane, implying rotational correlations between aromatic planes. Other polymeric compounds have been shown to build a biaxial phase [14, 15], as revealed by conoscopic investigations.

Disclinations in biaxial nematics show many similarities but also drastic topological differences with ordinary nematics [16] and since their theoretical analysis it has been a challenge to recognize the presence of biaxial nematics by their defects signature. But up to now, defect topological evidences for biaxiality are all wanting. Malthete and coworkers [17] have shown that the disclination lines of the biaxial compound discovered by Yu and Saupe [2] have a zigzag shape and have related this characteristic to biaxiality. However, it has been shown by Mihailovic and Oswald [18] that such a character also belongs to certain lines in usual uniaxial nematics. As far as thermotropic polymers are concerned, most of the optical studies [19-21] have shown the existence of thin threads (thins), sometimes linked to thick threads (thicks) : this is a classical observation also for small molecule nematics. One has to notice, however, that singular points have never been observed in thermotropic polymers : this is compatible with a biaxial behaviour since singular points are topologically unstable in biaxial nematics [22], but this might also be due to the large energy of such defects because of the anisotropy of the elastic constants. The main differences between small molecule nematics and thermotropic polymers show up in two facts : a) the thicks are as a rule less numerous in a polymer, because the large anisotropy of the elastic constants does not favour an « escape in the third dimension » (according to the expression coined by Meyer [23] ; b) there is a so-called « polydomain texture », which could be a high density defect texture [24-27] which does not call for biaxiality, but rather for long annealing times.

The conclusion is that even if there is some indication that high molecular weight thermotropic polymers could present some biaxiality, no clear evidence concerning their defect signature has been brought so far. We present here what we believe to be the first unambiguous observations of biaxial defects in a conventional thermotropic polymer.

2. Experimental section.

The polymer used in this work is a copolyesteramide supplied by Hoechst-Celanese and commercially known as Vectra B950®. The chemistry of this polymer was described by Calundann and Jaffe [28] and its composition is based on 60/20/20 2,6 hydroxynaphtoic acid/terephtalic acid/aminophenol.

i) Two types of samples were used : first, those obtained by peeling the skin of an extrudate made with a capillary rheometer (this produces highly oriented samples) whose thickness was between 20 and 100 μm ; secondly, samples obtained from injection molded plates whose thickness was *ca.* 1 mm. All samples were dried in an oven at 120 °C under vacuum for 24 hours to prevent hydrolytic chain scissions.

ii) Wide-angle X-ray diffraction studies (WAXD) were carried out by using a pinhole beam of Ni-filtered CuKα radiation ; diagrams were taken with a flat-film camera.

iii) Optical studies were carried out with a Leitz microscope used with a Linkam heating stage. Most of the observations were made under natural light except those for the measurements of birefringence which are done with sodium light ($\lambda_{Na} = 589$ nm) in conjunction with a Bereck compensator.

iiii) Magnetic field orientation studies were conducted by placing the samples in a heating stage made from high-purity copper foils and positioned between the poles of a water-cooled electromagnet. The field intensity was set at 2 T. The samples were quenched in water under the magnetic field for further WAXD studies.

3. Results.

3.1 OPTICAL OBSERVATIONS. — Two set-ups have been used : some peeled samples were placed on a single glass plate and others were placed between two untreated glass plates. Both types of samples were then heated up to 300 °C. For the first type of samples, there is no apparition of threads upon heating whereas for the second one, three classes of threads appear at 280 °C which have been classified as follows :

The threads of the first class scatter light very strongly and they appear as black thin threads under non-polarised light ; they are not sensitive to the direction of the polarisation of light. Two types of such threads have been observed : thins and thicks. Figure 1 shows a case where two thins are associated with a thick. The optical width of the core of the thin threads is relatively small and estimated to be less than 1 μm : this is the region where the propagation of light is strongly perturbed by scattering. The threads of this first class have all the characteristics of $S = \pm 1/2$ (thins) and $S = \pm 1$ (thicks) lines in usual nematics.

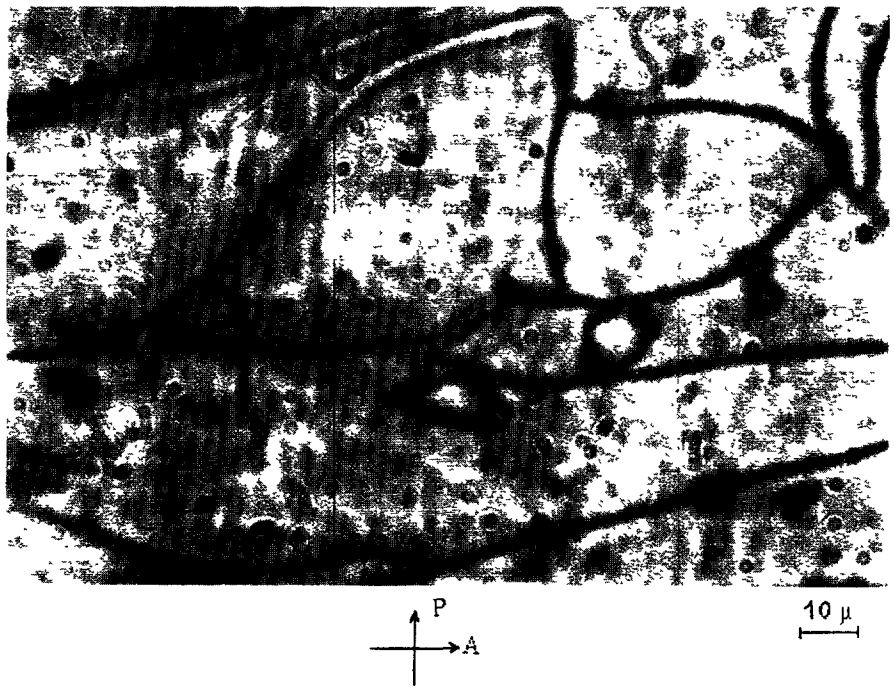

Fig. 1. — Highly scattering threads (class 1). Crossed polars.

The threads of the second class are the most numerous and have the following characteristic features :

— at first sight, they look thick but as seen later they are not the thicks of the first class described above ;

— they are weakly contrasted when viewed in non-polarised light (Fig. 2) ;

— they are perpendicular to the chain direction (remember that the peeled samples used are extremely well oriented) which is well defined as demonstrated by the strong extinction of the sample between crossed polars (Fig. 3) ;

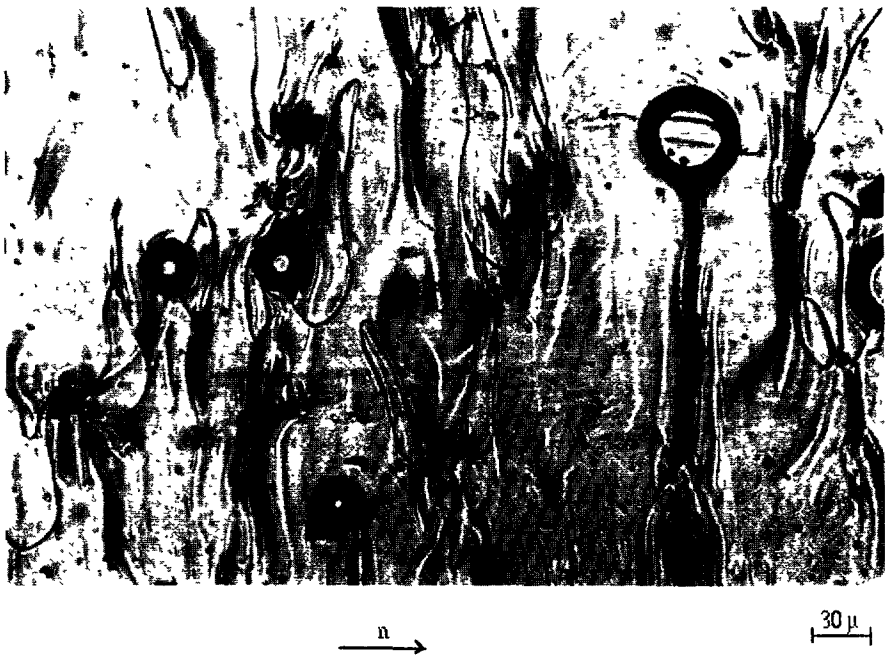

Fig. 2. — Weakly scattering threads (class 2) viewed under non polarised light. The chain orientation is horizontal. The black thin threads are the highly scattering threads of class 1 and the white thick threads are of class 2.

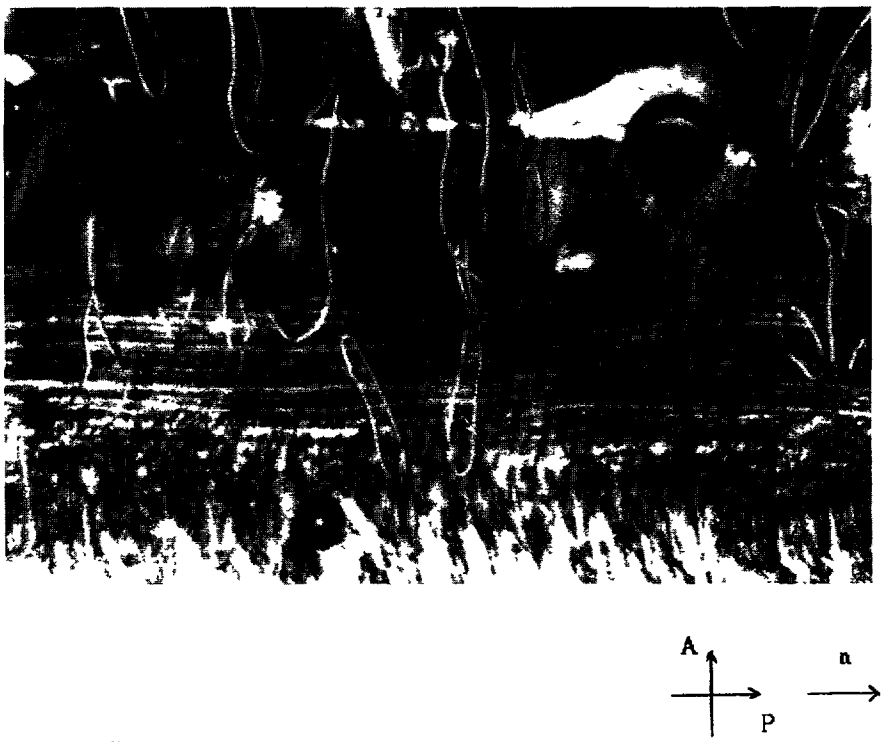

Fig. 3. — Same as figure 2 but with crossed polars.

— they disappear when the light is polarised perpendicularly to the chain direction (Fig. 4) and show up strongly when the light is polarised along the chain direction (Fig. 5) ;

— there is a strong dichroism located around the defect : light is strongly absorbed when it is polarised along the chain direction. The fact that the direction of maximum absorption is the chain direction is not surprising since it is so for all the organic compounds [29].

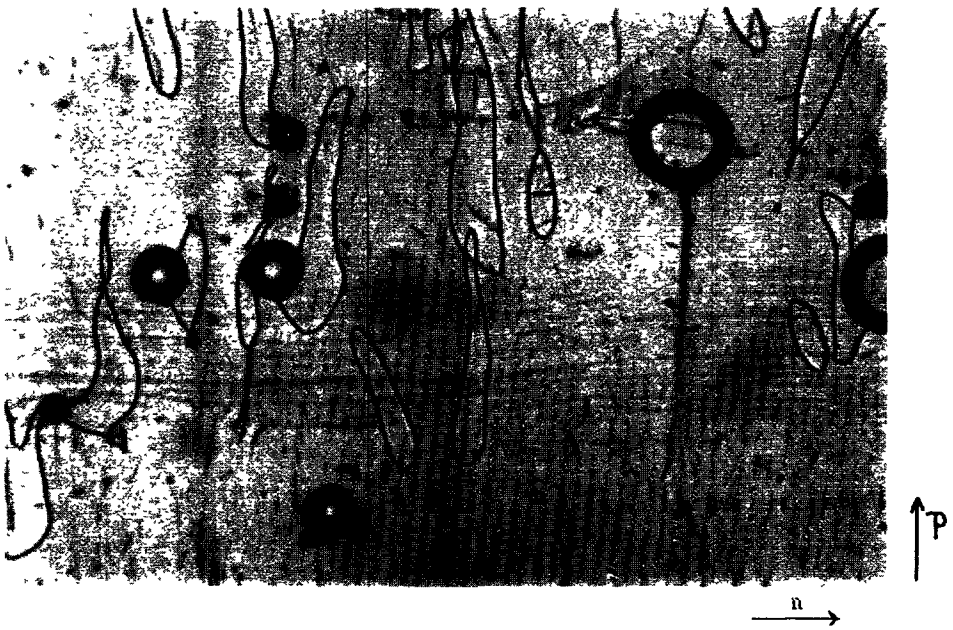

Fig. 4. — Same as figure 2 but for incoming light polarised along the chain direction.

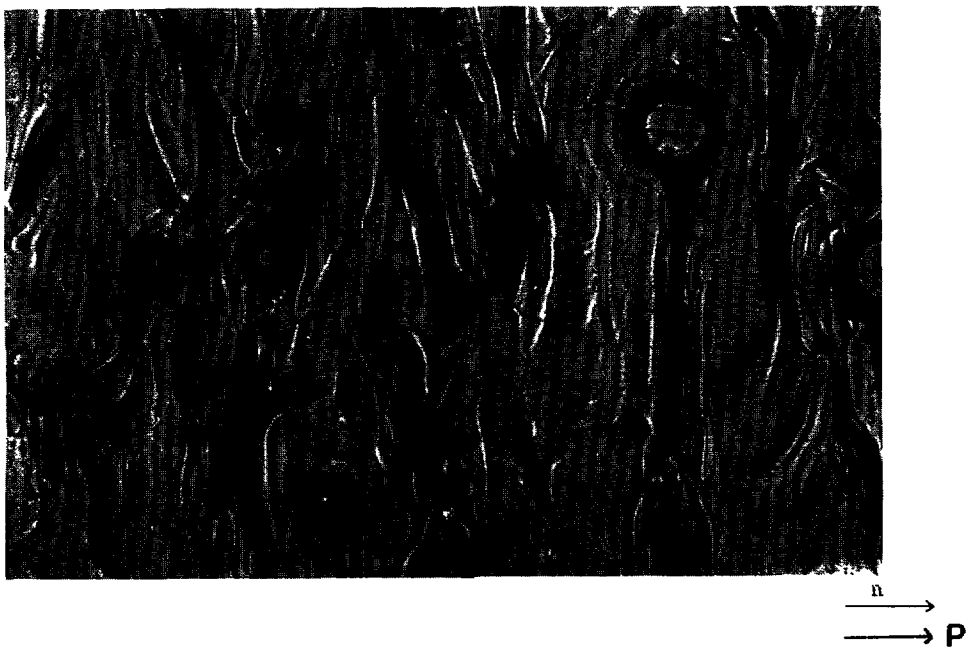

Fig. 5. — Same as figure 2 but for incoming light polarised perpendicularily to the chain direction.

The threads of the third class (moderately contrasted defects) are very few. They bear the optical features of both class 1 and class 2 defects : they are sensitive to the polarisation direction of light and give a strong local dichroism. One part of the thread is highly contrasted while the other part is weakly contrasted. Two threads of this class can be associated with another one of the same class (Figs. 6, 7 and 8).

Fig. 6. — Moderately contrasted defects viewed under non polarised light. The two arrows indicate a point of addition of such defects.

Fig. 7. — Same as figure 6 but for incoming light polarised along the chain direction.

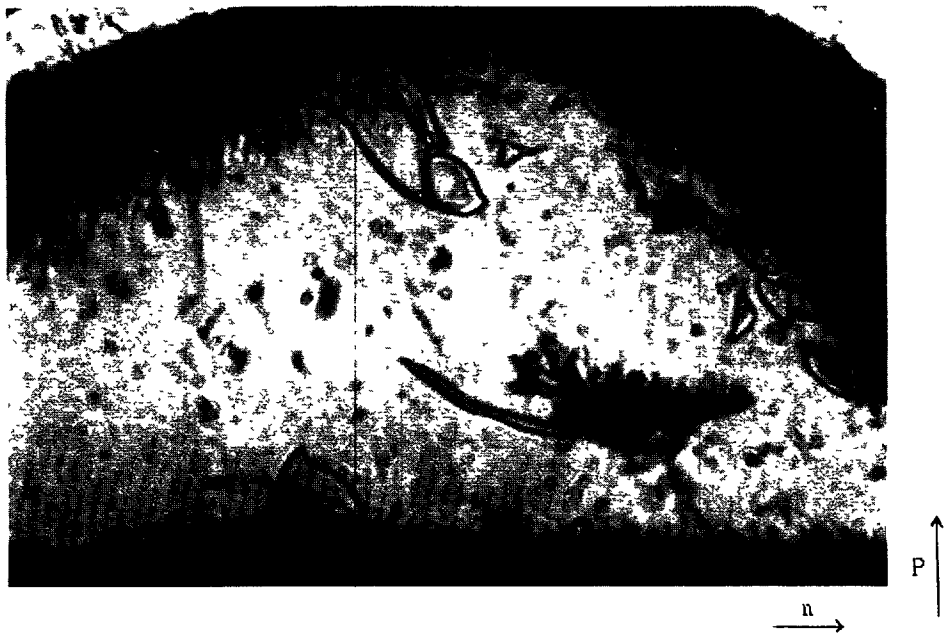

Fig. 8. — Same as figure 6 but for incoming light polarised perpendicularly to the chain direction.

The most interesting is the fact that three threads, each of them belonging to a different class, can meet. This is demontrated in figures 9, 10 and 11 where one part of the disclination loop is a class 1 thread which is transformed into a class 2 plus a class 3 thread at points A and B (see Fig. 9). It has been checked that the points of encounter really exist by moving the top glass plate : point A, say, moves and each thread follows its motion, proving that at point A, the threads are linked physically.

These results show very unusual observations and have never been reported for uniaxial nematics. It seems then necessary to know whether this polymer is biaxial : one way is to study the orientational behaviour of the material under a magnetic field. As a magnetic field can induce a distortion of the long axis of the molecules (due to the fact that each aromatic plane orients itself in order to contain the field lines), it should be possible to induce distortion of the other two short axes of the chains (those describing the orientation of the aromatic planes), provided that the experimental parameters are correctly chosen.

3.2 ORIENTATIONAL BEHAVIOUR UNDER A MAGNETIC FIELD. — The experimental configuration (Fig. 12) is the first Freederick's geometry, as mentioned by de Gennes [30] and allows in principle for a determination of K_1.

As demonstrated by the WAXD fiber diagram of a thick sample (thickness : 1 mm) held under a magnetic field of 2 T at 300 °C during 2 hours, the chains orient towards the field lines (Fig. 13). The corresponding diagram of a thin sample (thickness : 20 μm) is totally different and shows no tilt of the chain director (Fig. 14). However, the evolution of the birefringence of these thin samples increases strongly in the course of time (Fig. 15) : after about one hour, a maximum is reached.

When a uniformly oriented sample is placed in a magnetic field, a distortion appears above a critical field H_c whose value is predicted by the Frank-Oseen theory :

$$H_c = \frac{\pi \sqrt{K_1/\chi}}{d} \tag{1}$$

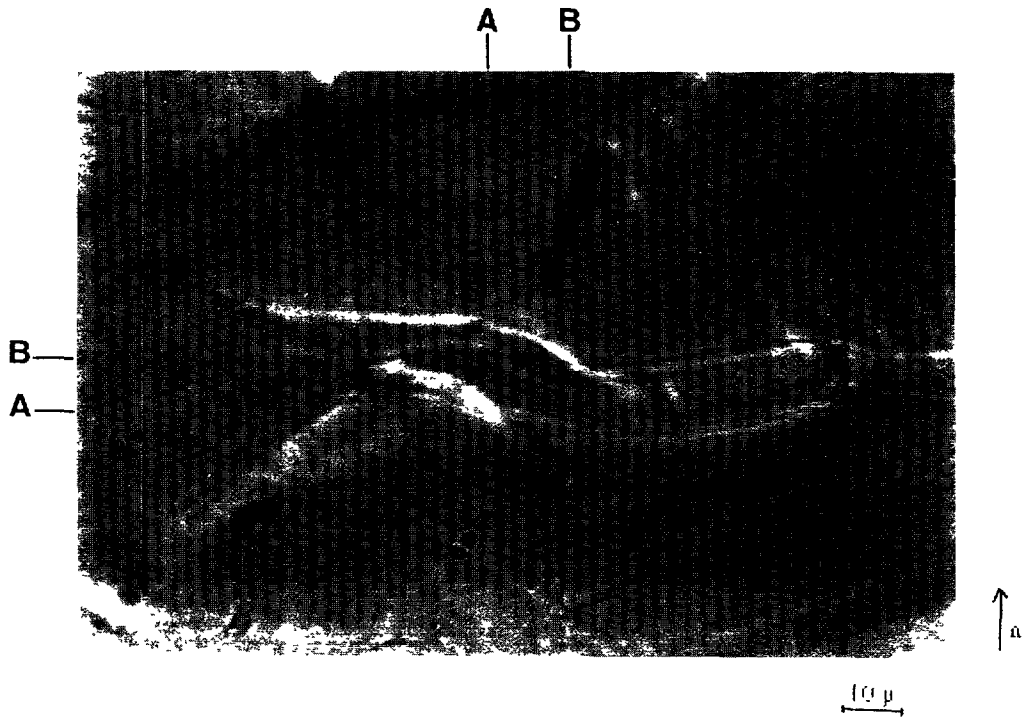

Fig. 9. — Disclination loop viewed under non polarised light. The chain orientation is vertical. Points A and B are connecting points of three different threads (see text).

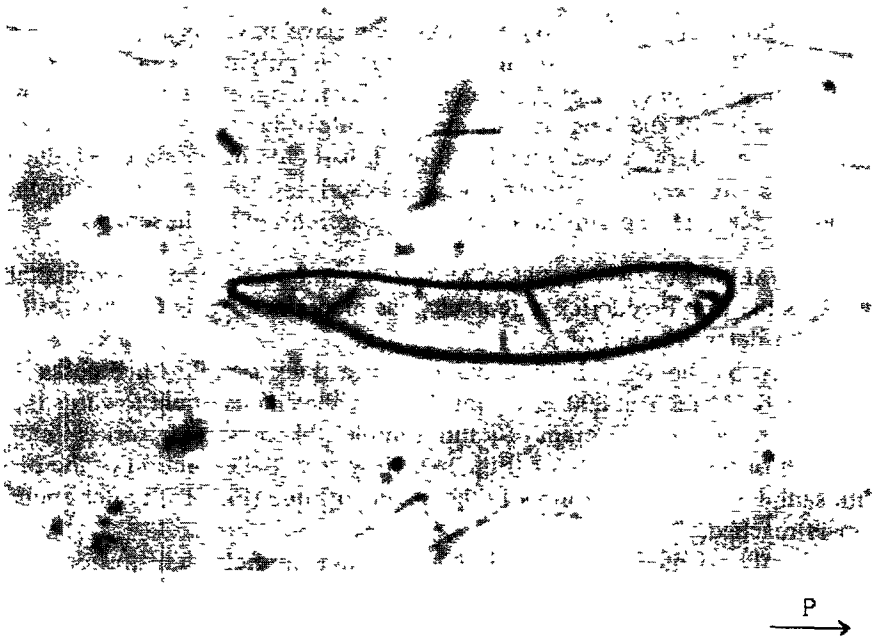

Fig. 10. — Same as figure 9 but for incoming light polarised perpendicularly to the chain direction.

Fig. 11. — Same as figure 9 but for incoming light polarised along the chain direction.

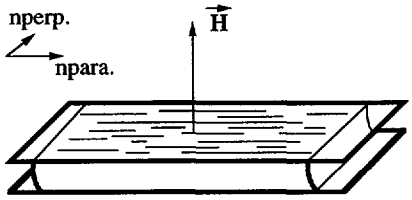

Fig. 12. — Configuration of the samples placed under a magnetic field H. n_{para} and n_{perp} are respectively the measured refractive indices parallel and perpendicular to the chain direction.

where d is the sample thickness, K_1 the first Frank elasticity constant and χ the anisotropic part of the magnetic susceptibility.

Equation 1 predicts that the critical field for the thin samples is twenty times that necessary for the thick samples : it is then likely that the actual critical field for the thin samples is much higher than 2 T. Birefringence, however, increases, which is an indication of a reorientation of the aromatic planes. Let us call n_x, n_y and n_z the three principal refractive indices of an aromatic plane in a copolyester chain (Fig. 16). It is considered that the contribution of the other bonds of the chain (that of the ester and amide functions) to the variation of birefringence is negligible since their transverse polarisabilities α_x and α_z are equal. As classically reported by some authors [11, 27], the following inequality holds : $n_z < n_x < n_y$ which implies $\alpha_z < \alpha_x < \alpha_y$ since there is the Lorenz-Lorentz relationship between any N_i and α_i .

$$(n_i^2 - 1)/(n_i^2 + 2) = K \cdot \alpha_i \text{ where } K \text{ is a material constant.} \quad (2)$$

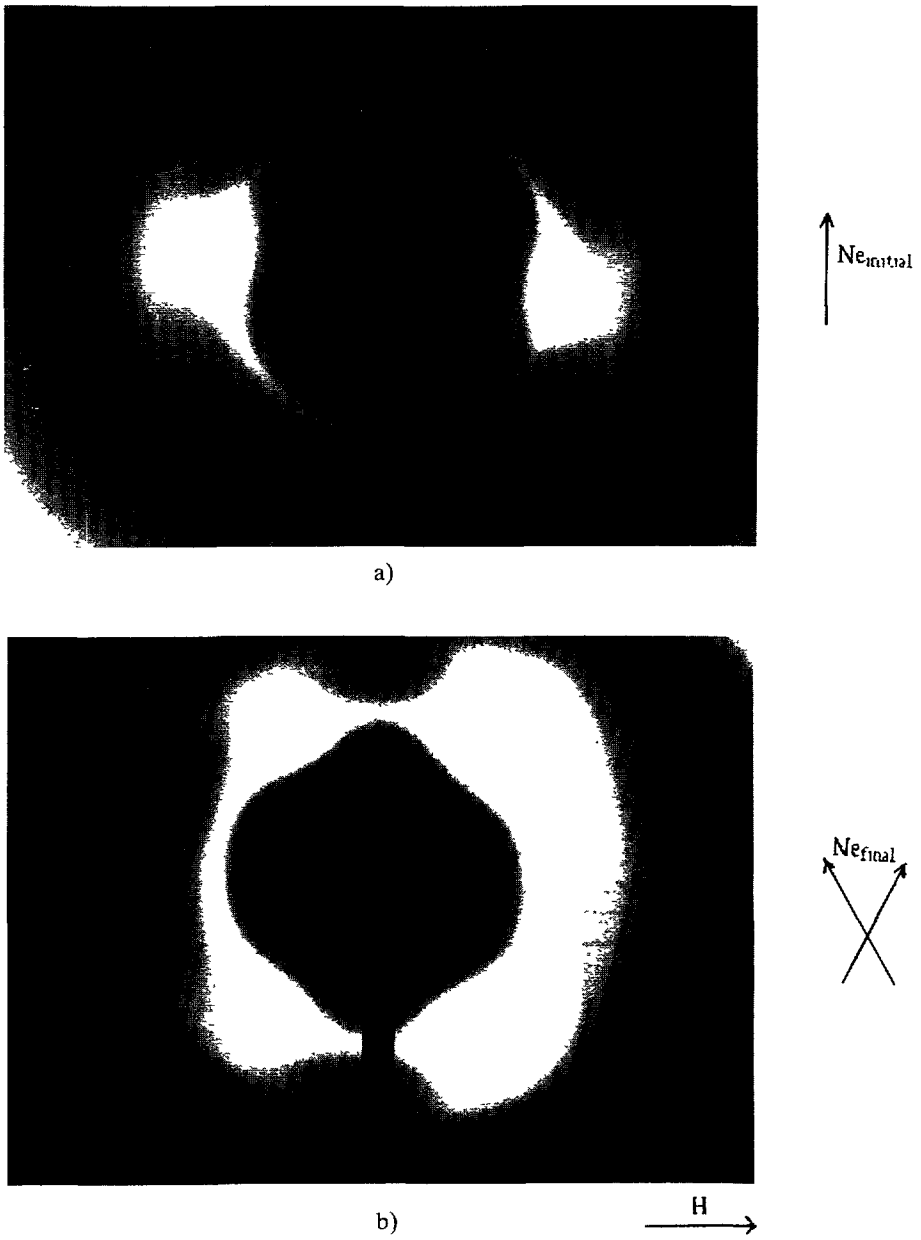

Fig. 13. — WAXD fiber diagram of a thick sample held at 300 °C during 2 hours. a) Without the magnetic field. b) With the magnetic field.

Assuming that before the field application the aromatic planes are not oriented to contain the magnetic field lines (Θ is different from $\pi/2$ in Fig. 17), there will be a decrease in $\alpha_{perp.}$ during the field application (since Θ will tend towards $\pi/2$ and then $\alpha_{perp.}$ will tend towards α_z) implying a decrease in the refractive index $n_{perp.}$. Since the other refractive index n_{para} remains unchanged and equal to n_y, the measured birefringence Δn will increase where :

$$\Delta n = n_{para.} - n_{perp.} = n_y - n_{perp} \ . \tag{3}$$

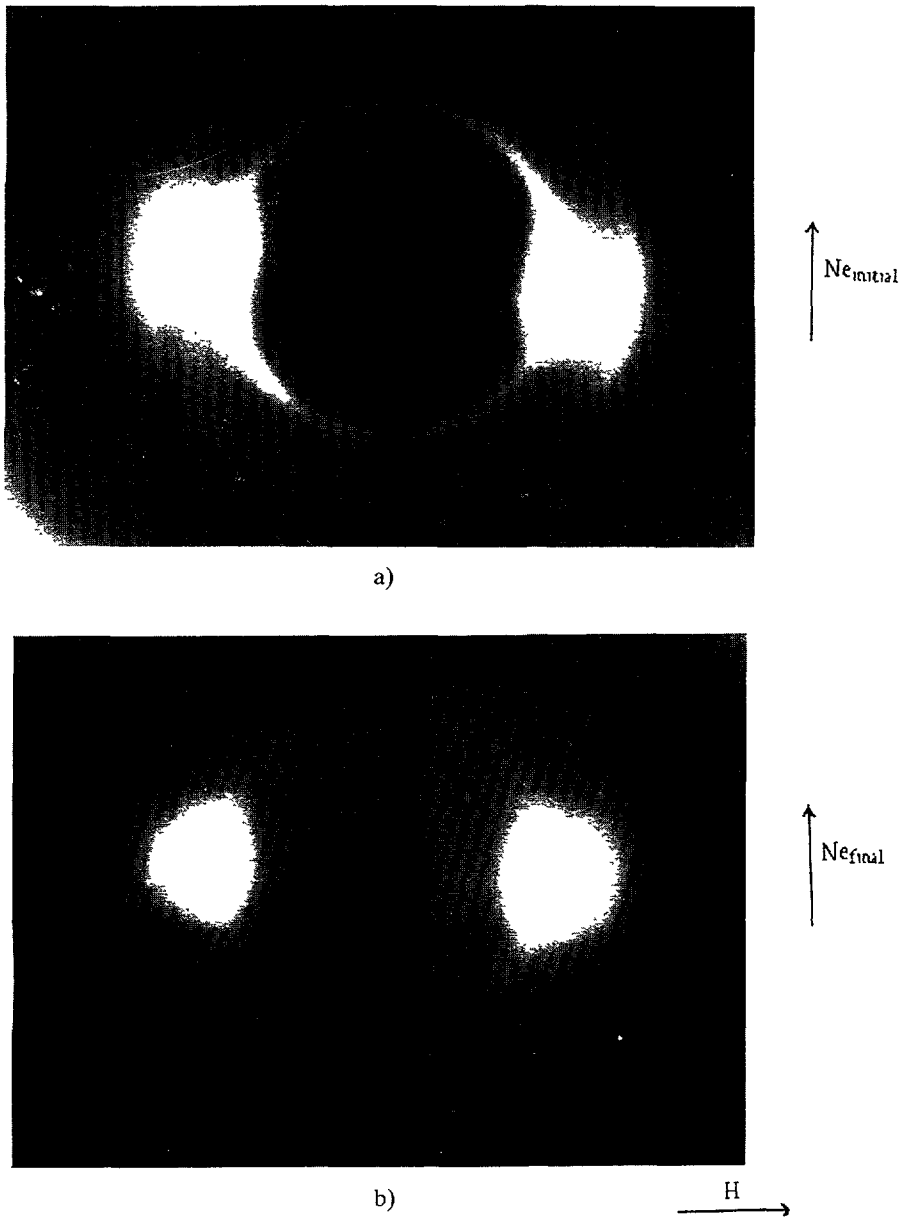

Fig. 14. — WAXD fiber diagram of a thin sample held at 300 °C during 2 hours. a) Without the magnetic field. b) With the magnetic field.

A magnetic field strength of 2 T is then below the critical field necessary to orient the chains but appears experimentally above the critical field to rotate the aromatic planes. This is typical of a biaxial behaviour since two regimes of orientation exist. However we do not claim that this biaxial behaviour is an intrinsic property of this polymer since it is possible that the same average orientation of the aromatic planes so far obtained could be due only to the influence of the magnetic field. But let us remark a) that any birefringence obtained under the action of a magnetic field does not decrease as the sample is heated up again to 300 °C without

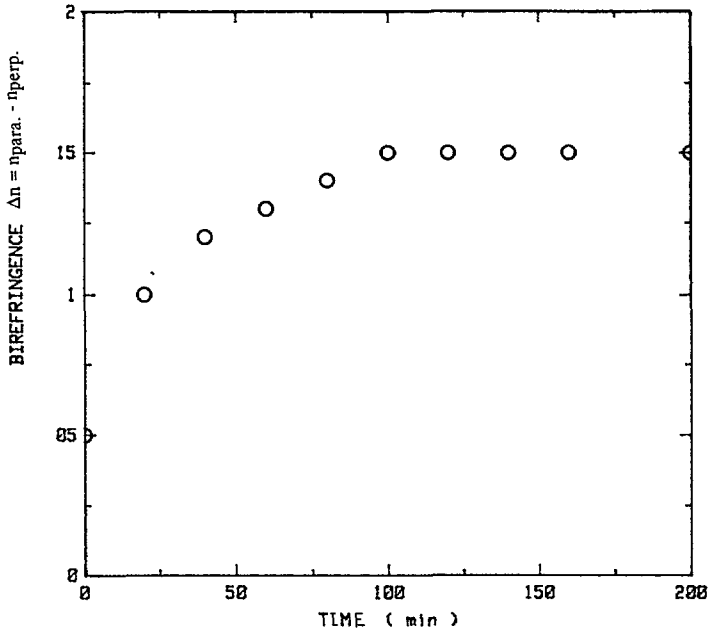

Fig. 15. — Evolution of birefringence with respect to time for the thin sample held at 300 °C under the magnetic field.

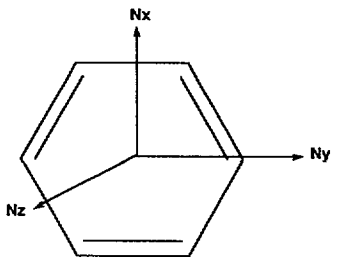

Fig. 16.

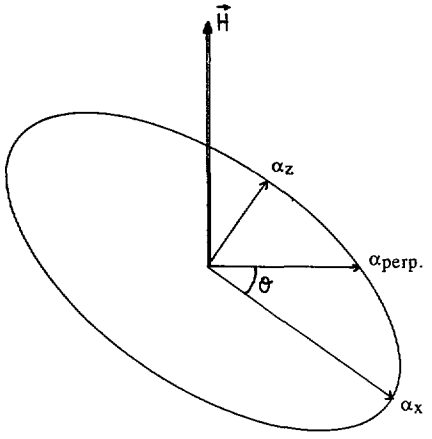

Fig. 17.

Fig. 16. — Definition of the three principal refractive indices of an aromatic plane in a polyester chain.

Fig. 17. — Polarisability ellipse of the aromatic plane of figure 16. Z axis is perpendicular to the aromatic plane XY which is rotated of an angle θ from the plane perpendicular to the magnetic field vector H (see Fig. 12).

the magnetic field ; b) that the defects do anneal in samples which have a free surface, an effect which could be due of course to the attractive image forces acting on the sample, without invoking a breaking of the true biaxial phase ; c) that defects persist in samples located between glass plates ; d) that the X-ray experiments we have conducted up to now are

not precise enough to test biaxiality unambiguously (results obtained in that way will be published in a next paper [33]). It can therefore be inferred at this point that the observed biaxiality could be induced by anchoring forces. We leave the problem open at this stage.

4. Discussion.

4.1 MODEL OF DEFECTS. — As already stated, the defects of the first class can be explained on the basis of uniaxiality. Then, if the weakly scattering defects of the second class were typical of uniaxility, they should be classified as thick. However those thicks would be very different from the highly scattering thicks of the first class which never disappear for a particular direction polarisation and are not as a rule perpendicular to the chain direction. It could be a possibility that these are non-singular thick threads (by escape in the third dimension), but this would require a rather peculiar type of anisotropy of the Frank constants, since it is well-known that integer lines are generally singular for this very anisotropy [26]. This is incompatible with the fact that these are the most numerous defects. It then appears that the weakly contrasted defects of class 2 cannot enter the same topological class as the highly scattering thicks, which means that they are to be classified as a particular class of biaxial defects. It is recalled again that the biaxiality of this nematic phase could be the consequence of external elastic forces such as those induced by the glass surface, orienting the aromatic planes parallel to it. The biaxial state thus obtained is perhaps not the one that this polymer would adopt if it were free from wall influence. As far as the samples used here are concerned, biaxiality is high enough to give defects typical of it and, as such, the medium is biaxial.

Let us now discuss in some details the nature of the observed defects in the light of biaxiality. The biaxial character of a medium is defined by three different directors along three orthogonal directions. For the sake of simplicity, it will be considered that these correlations are perfect, that is to say that the aromatic planes are all parallel. Under this assumption, the chain will be modelled as a thin ribbon (Fig. 18) and no difference will be made between the local order parameter of the chain itself and the macroscopic medium.

In such a biaxial medium, three types of half integer disclination lines can be defined due to the fact that there are three possibilities of discontinuity, one director remaining unchanged.

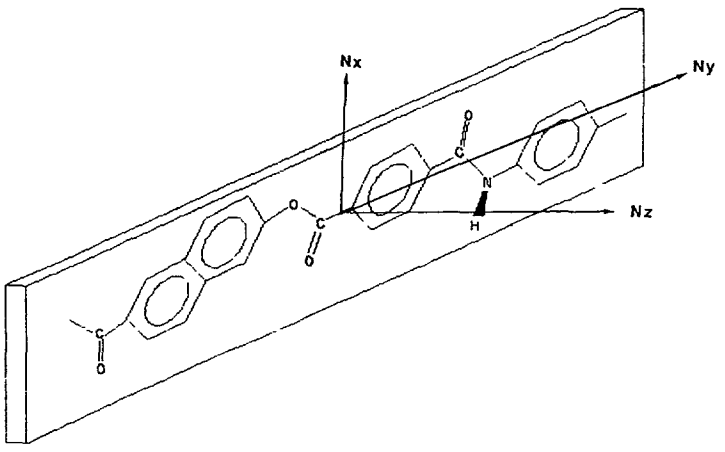

Fig. 18. — Structural model of the chain. N_x, N_y and N_z are the three principal refractive indices.

In figure 19, twist disclinations are represented whereas wedge disclinations are shown in figure 20. It is worth noting that the E_y line is parallel to the main director Y in the wedge case whereas it is perpendicular to it in the twist case. Let us assume now that the observed lines are twist lines. These defects can be classified (Tab. I) with respect to their light scattering properties, bearing in mind that the more chain ends are present in the core of the defect, the higher is the scattering [32] and that, for an equivalent number of chain ends, the higher the discontinuity of the refractive indice, the higher the scattering. In this respect, we expect few chain ends clustered in the core of the defects of the second class, especially if the disclinations are twist disclinations. It is then likely that the observed lines are twist lines since in this case only, it is possible to define a defect line with few chain ends in the core and which is perpendicular to the main director Y.

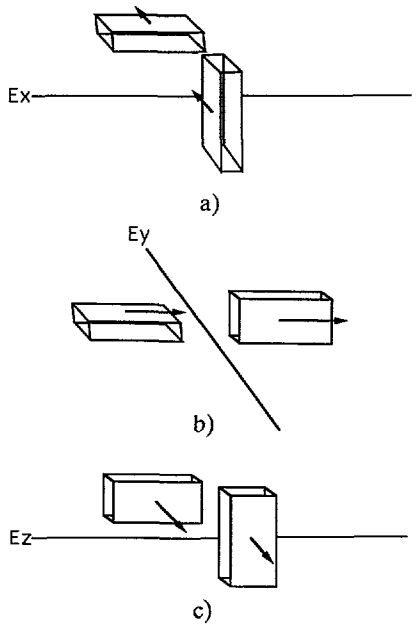

Fig. 19. — Model of the three possible half integer twist disclination lines in a biaxial nematic. a) E_x defect. b) E_y defect. c) E_z defect.

The existence of these three types of defects points to the presence of a biaxial behaviour ; the topological theory of disclination lines for biaxial nematics classifies them indeed as the elements of the quaternion group Q which is a non-abelian group of 8 elements (see Table II). The elements E_x, E_y, E_z and their inverses correspond to the three types of thin lines seen above, the thick lines belonging to the common class called $-I$ in table II.

It is well known that in uniaxial nematics « two thins give one thick ». The same is true in biaxial nematics, according to some of the multiplication rules of table II : E_i times E_i gives $-I$. E_i is indeed a line about which the j and k directors (j and k being different from i) suffer a rotation of π. $A - I$ line is a line about which the same directors rotate by an angle of 2 π, but it is possible to transform smoothly a 2 π line involving two prescribed directors in a 2 π line involving two other directors. Contrarywise, it is not possible to transform continuously an E_i line into an E_j line, so that there are three types of independent π lines (i.e. of strength $S = \pm 1/2$) in a biaxial nematic. Each type of line behaves much like a line in a

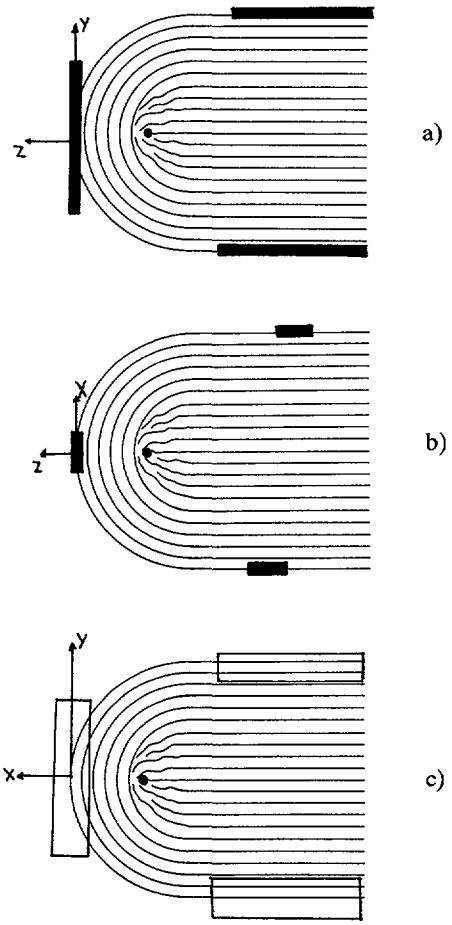

Fig. 20. — Model of the three possible half integer wedge disclination lines in a biaxial nematic. a) E_x defect. b) E_y defect. c) E_z defect.

Table I. — *Scattering of light by the three types of defects shown in figure 19. The classification of the defects on the right column refers to the one given at the beginning of the « Results » section.*

Defect type	Value of refractive indice discontinuity	Density of chain ends	Scattering of light	Defect class
E_1	N_y-N_z : high	high	high	1
E_2	N_x-N_z : medium	low	weak	2
E_3	N_y-N_x : small	high	medium	3

uniaxial nematic, with some differences which are worth mentioning : while the lines $S = + 1/2$ and $S = - 1/2$ are topologically identical in a uniaxial nematic, this is not true in a biaxial one ; hence the product of the lines of opposite strengths $E_i(S = + 1/2)$ and $E_i^{-1}(S = - 1/2)$ is a zero line, but the product E_i^2 is a $- I$, which is a topologically stable line

Table II. — *Multiplication rules for biaxial defects.* E_x, E_y, E_z *and their inverses* E_x^{-1}, E_y^{-1}, E_z^{-1} *correspond to the three possible types of thin lines, the thick lines belonging to the only class* $-I$.

I	$-I$	E_x	E_y	E_z	E_x^{-1}	E_y^{-1}	E_z^{-1}
$-I$	I	E_x^{-1}	E_y^{-1}	E_z^{-1}	E_x	E_y	E_z
E_x	E_x^{-1}	$-I$	E_z	E_y^{-1}	I	E_z^{-1}	E_y
E_y	E_y^{-1}	E_z^{-1}	$-I$	E_x	E_z	I	E_x^{-1}
E_z	E_z^{-1}	E_y	E_x^{-1}	$-I$	E_x^{-1}	E_x	I
E_x^{-1}	E_x	I	E_z^{-1}	E_y	$-I$	E_z	E_y^{-1}
E_y^{-1}	E_y	E_z	I	E_x^{-1}	E_z^{-1}	$-I$	E_x
E_z^{-1}	E_z	E_y^{-1}	E_x	I	E_y	E_x^{-1}	$-I$

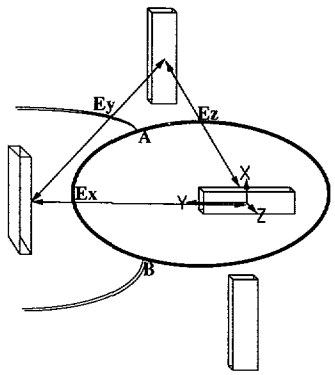

Fig. 21. — Illustration of the orientation of the thin ribbons around three different types of half integer twist disclination lines corresponding to the optical features of figures 9, 10 and 11.

(i.e. singular on two directors) ; the lines which escape in the third dimension are 4 π lines in a biaxial nematic (we have no convincing observations of such lines) ; finally, since there are three types of topologically equivalent $-I$ lines (the most general $-I$ line is a mixture of those), the type which prevails in the static situation is the one which involves the smaller free energy, i.e. the one which is singular on the « weakest » directors, letting the third one to « escape in the third dimension ». This is the reason why we see only one type of $-I$ lines, and this type has all the appearance of a thick in a uniaxial nematic. However, the necessity of letting the strong director (which is with no doubt along the molecular elongation) alone to « escape » imposes some constraint on the shape of the line or the overall orientation of the chains. The resulting geometry is such that the $-I$ lines are twist lines, with the strong director essentially perpendicular to the lines, except in their close vicinity, where this change of orientation (the « escape ») is evidenced by a strong pleochroism as in figure 5.

According to table II, another possibility of topological multiplication rule is « E_i times E_j gives an E_k line » ($i \neq j \neq k$). This statement, which has no equivalent in uniaxial nematics, is illustrated in figure 9 where three different threads meet at points A and B. This observation is of course the simplest and most convincing signature of biaxiality in a static sample. In figure 21 is shown the orientation of the thin ribbons around each defect, highlighting the necessity of having two meeting points.

4.2. RHEO-OPTICAL STUDIES. — The non-abelian character of the quaternion group Q should in principle show up in dynamical experiments : since $E_i \,.\, E_j \neq E_j \,.\, E_i$, there is an « obstruction » [16] to the crossing of two π lines of different indices ($i \neq j$), and an imposed crossing should result in the formation of a $-I$ line joining the two π lines after they have crossed each other. Unfortunately, we have not yet been able to observe this effect, which probably has a large occurrence only at high shear deformation when a worm texture is developed, and for which a direct observation is difficult. At 300 °C, when the upper plate is moved in a direction parallel to the chain ones, two separate events occur :

— first, at low shear deformation, a splitting of the E_y disclination lines into an E_x plus an E_z lines (Figs. 22 and 23) ;

— in a second step, at higher shear deformation, a multiplication of the E_x and E_z lines yields the so-called worm texture [24]. The splitting of the E_Y threads could be interpreted in terms of a rotation of the chains located in the vicinity of the defect, the chains being far from it remaining unperturbed : this difference in behaviour shows that the instability is higher near the core of the defect during the shear (Fig. 24) which implies the creation of an E_x and an E_z defects. The fact that the E_y defects are broken first shows that the energy stored in them is the lowest, which is not surprising due to the weakest distortion involved.

4.3 COMMENTS ON THE ORIGIN OF THE OPTICAL CONTRAST. — The reader has already noticed that we have interpreted the image contrast as if the sample behaved optically as an uniaxial medium, with $N_e \approx N_y$, $N_o \approx N_x$, N_z. In particular we did so for the contrast of the threads of the second class, which are out of contrast in figure 4, and strongly contrasted in figure 5. In figure 4, the plane of polarisation is perpendicular to the chains and the propagating wave would be the ordinary one ($N = N_o$) which remains ordinary when crossing the sample ; hence its geometrical path remains rectilinear, even if the nematic is deformed. In figure 5, the plane of polarisation is along the chains and the propagating wave is extraordinary ($N = N_e$ at the entrance boundary), so that it changes refraction index when crossing the sample under the action of any deformation ; more precisely, its geometrical path obeys the Fermat principle ($\int N \,.\, d\ell$ is an extremum) and its plane of polarization rotates accordingly. Hence a contrast shows up under crossed polars.

In the analysis which follows, we shall assume that the biaxiality is small, i.e. we have :

$$N_x = N_o + \eta \,, \qquad N_z = N_o - \eta \tag{4}$$

where η is some small positive quantity. Also, N_y is larger than N_x and N_z. Hence the equation of the index surface, which is written when there is no approximation :

$$x^2/N_x^2 + z^2/N_z^2 + y^2/N_y^2 = 1 \tag{5}$$

is now written

$$(x^2 + z^2)\,(1 + 3\,\eta^2/N_o^2)/N_o^2 - 2\,\eta\,(x^2 - z^2)/N_o^3 + y^2/N_e^2 = 1 \tag{6}$$

where we have adopted the notation $N_y = N_e$.

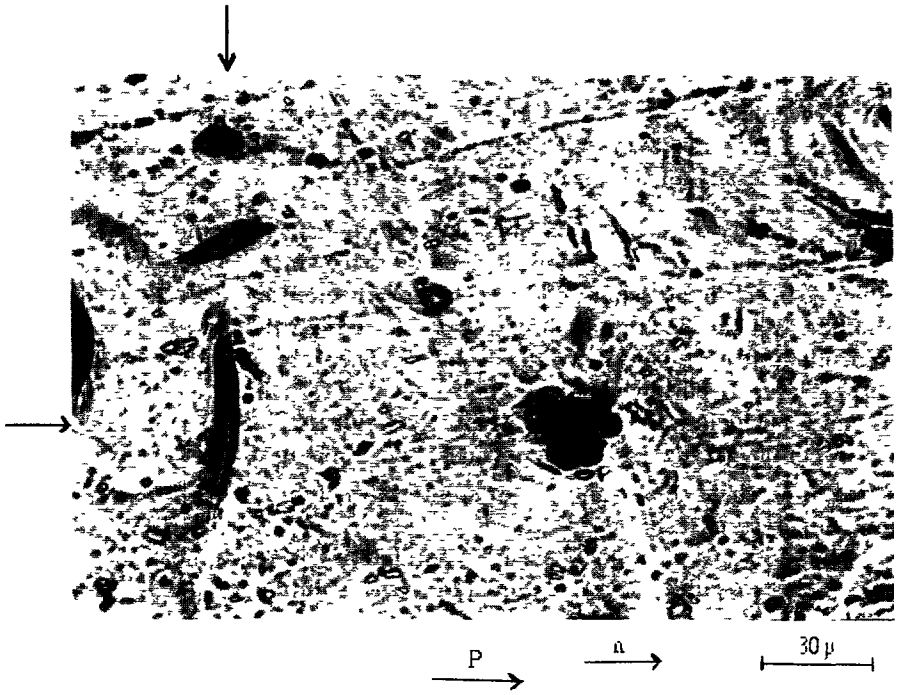

Fig. 22. — E_3 defect denoted by the two arrows before shear for the incoming light polarised perpendicularly to the chain direction which is horizontal.

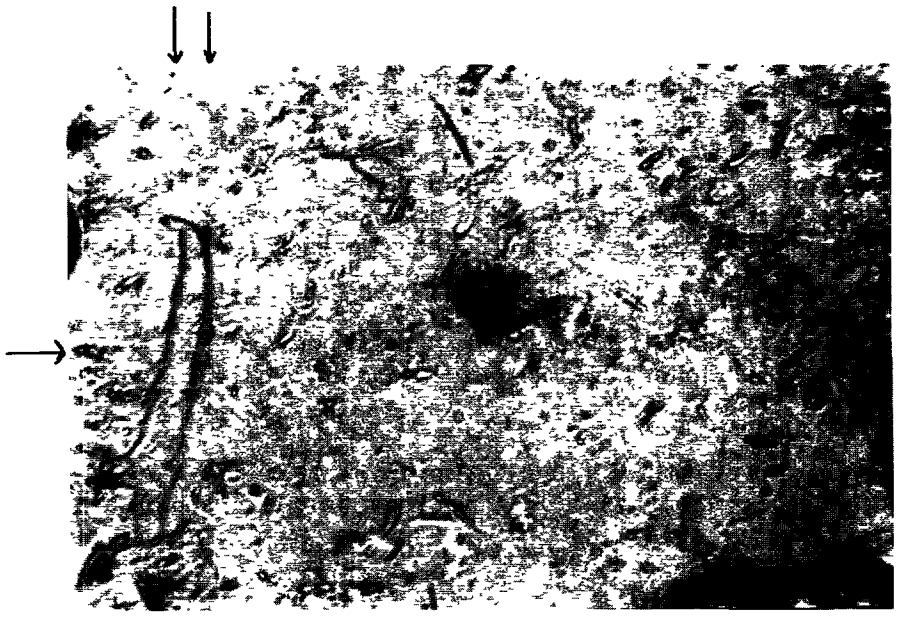

Fig. 23. — Creation of an E_1 and an E_2 defects denoted by the three arrows after shear parallel to the chains direction viewed under non polarised light.

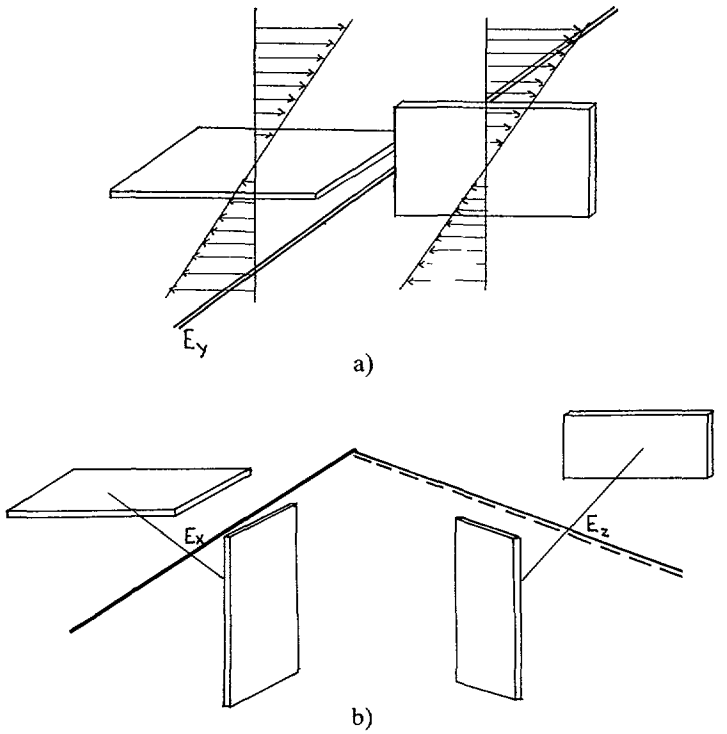

Fig. 24. — Behaviour of an E_y defect during shear. a) Configuration before shear. b) Configuration after shear.

Let us first consider an incoming ray of wave vector **k** perpendicular to the chain « average » direction. Take $\mathbf{k} = k$ (cos φ, 0, sin φ). φ is here the rotation angle of the phenyl groups. The cross-section of the index surface by a plane perpendicular to **k** is an ellipse (the ellipse of polarisation) whose major and minor axes are along the electric displacement vectors $\mathbf{D}_1$ and $\mathbf{D}_2$ in which the incident light splits. The major axis is still along the y direction, and its half-length N_y gives the value of the refraction index of the corresponding polarised wave, which is similar to the extraordinary wave of the uniaxial case. The other polarisation, which is still in a plane perpendicular to the molecules, has refraction index :

$$1/N^2 = \sin^2 \varphi/N_x^2 + \cos^2 \varphi/N_z^2 \approx 1/N_o^2 + \eta \sin 2\varphi/N_o^3 \tag{7}$$

and behaves like an ordinary wave, especially if some averaging process makes the term in sin 2 φ either zero or constant.

Let now the main chain rotate about the x- or the y-directors. **k** makes an angle $\pi/2 - \theta$ with the plane x, z.

$$\mathbf{k} = k(\cos\theta \cos\varphi \; ; \sin\theta \; ; \cos\theta \sin\varphi) \, . \tag{8}$$

We introduce a set of orthogonal axes linked to **k**, and write the equation of the index surface in these new axes. We take the X axis along **k** and the two other axes in the plane $X = 0$, which is the plane which intersects the ellipsoid along the new ellipse of polarisation :

$$\begin{aligned} X &= x \cos\theta \cos\varphi + y \sin\theta + z \cos\theta \sin\varphi \\ Y &= x \sin\theta \cos\varphi - y \cos\theta + z \sin\theta \sin\varphi \\ Z &= x \sin\varphi - z \cos\varphi \end{aligned} \tag{9}$$

and make the change of coordinates :

$$\begin{aligned} x &= (X \cos\theta + Y \sin\theta)\cos\varphi + Z \sin\varphi \\ y &= X \sin\theta - Y \cos\theta \\ z &= (X \cos\theta + Y \sin\theta)\sin\varphi - Z \cos\varphi \,. \end{aligned} \tag{10}$$

We now express the equation of the index surface in these new coordinate system, and make $X = 0$; this yields, to first order in η :

$$Y^2(\sin^2\theta/N_o^2 + \cos^2\theta/N_e^2) + (1 + 2\,\eta\cos\varphi/N_o)\,Z^2/N_o^2 - 4\,YZ\eta\sin 2\varphi\sin\theta/N_o^3 = 1 \tag{11}$$

This is the ellipse of polarisation, of general form $Y^2u^2 + Z^2v^2 - 2\,YZw = 1$. Its axes are at an angle χ of the Y and Z axes, with :

$$\tan 2\chi = 2\,w/(v^2 - u^2) = 2\left\{\eta N_e^2/N_o(N_o^2 - N_e^2)\right\}\sin\theta\sin 2\varphi/\cos^2\theta + O(\eta^3) \tag{12}$$

$\tan\chi$ is of first order in η and in $\sin\theta$: we write $\tan 2\chi = 2\lambda\eta\sin\theta$ and get :

$$\cos^2\chi = 1 - \lambda^2\eta^2\sin^2\theta + O(\eta^4)\,, \qquad \chi = \lambda\eta\sin\theta + O(\eta^3)\,. \tag{13}$$

The director cosines of the polarisations are the coefficients of the formulae of transformation from the set of axes x, y, z to the set $x' = Y\sin\chi - Z\cos\chi$, $y' = Y\cos\chi + Z\sin\chi$, X. We get :

$$\mathbf{D}_{x'} \approx (\sin\chi\cos\varphi\cos\theta - \sin\varphi\cos\chi,\ \sin\chi\sin\theta\,,\ -\sin\chi\sin\varphi\cos\theta - \cos\varphi\cos\chi)$$

$$\mathbf{D}_{y'} \approx (\cos\chi\cos\varphi\cos\theta + \sin\varphi\sin\chi,\ \cos\chi\sin\theta\,,\cos\chi\sin\varphi\cos\theta - \cos\varphi\sin\chi)\,.$$

The remarkable fact about these formulae is that the polarisation $\mathbf{D}_{x'}$ keeps practically perpendicular to the y-direction, since $\sin\chi\sin\theta$ is so small, of order $\eta\theta^2$ as long as the rotation θ of the main chain is small. Hence its « ordinary » character is not much modified by the distorsion. This is all the more so that its propagation does follow the Fermat principle, so that its optic-geometrical path does not curve as quickly as the director rotates. On the second hand, its « ordinary » character is not modified either if η is small. These reasons add to explain why the defects of the second class are practically out of contrast with light polarised perpendicular to the chains.

5. Conclusion.

Optical observations of the thread texture of the VECTRA B950® nematic polymer have shown the existence of three types of half integer disclination lines, called E_x, E_y and E_z.

Although the scattering of light is strong for E_x and E_z due to the presence of chain ends in the core, it is not so for E_y lines which disappear for a chain perpendicular direction polarisation of the incident light. Calculations show that this is due to the fact that the character of this incoming light is not modified if biaxiality is weak, implying that the rotational correlations of the aromatic planes between neighbouring chains are probably weak : it is not clear at the present time whether this property is intrinsic or not, since it is likely that the influence of the glass surfaces on the samples could be far from negligible. These correlations give rise to a strong dichroism localised near the E_y and E_z defects, an effect which will be further investigated in a forthcoming paper [33].

This is the first nematic polymer for which the knowledge and classification of the defects have permitted us to show that biaxiality is involved. Moreover, it gives the opportunity to

define the motion of these defects under a shear flow. The first result obtained is the existence of two regimes : a splitting of the E_y defects into an E_x plus an E_z defect at a shear deformation lower to that corresponding to the multiplication of the E_x and the E_z defects. Further studies are conducted to investigate the nature of the worm texture defects, concerning especially the prediction of large $-I$ defect density due to the non-abelian character of the quaternion group Q.

References

[1] FREISER M. J., *Phys. Rev. Lett.* **24** (1970) 1041.
[2] YU L. I., SAUPE A., *J. Am. Chem. Soc.* **102** (1980) 4879.
[3] PRAEFCKE E., KOHNE B., SINGER D., DEMUS D., PELZI G., DIELE S., *Liq. Cryst.* **7** (1990) 589.
[4] HESSEL F., HERR R. P., FINKELMANN H., *Makromol. Chem.* **188** (1987) 1597.
[5] PRAEFCKE K., KOHNE B., GUNDOGAN B., *Mol. Cryst. Liq. Lett.* **7** (1990) 27.
[6] CHANDRASEKHAR S., RATNA B. R., SADASHIVA B. K., RAJA V. N., *Mol. Cryst. Liq. Cryst.* **165** (1988) 123.
[7] CHANDRASEKHAR S., SADASHIVA B. K., RATNA B. R., RAJA PRAMANA V. N., *J. Phys.* **30** (1988) L491.
[8] PRAEFCKE K., KOHNE B., GUNDOGAN B., SINGER D., DEMUS D., DIELE S., PELZL G., BAKOWSKY U., *Mol. Cryst. Liq. Cryst.* **198** (1991) 393.
[9] DONALD A. M., WINDLE A. H., *J. Mat. Sci.* **18** (1983) 1143.
[10] VINEY C., MITCHELL G. R., WINDLE A. H., *Polym. Commun.* **24** (1983) 145.
[11] VINEY C., DONALD A. M., WINDLE A. H., *Polymer* **26** (1985) 870.
[12] WINDLE A. H., VINEY C., GOLOMBOK R., DONALD A. M., MITCHELL G. R., *Faraday Discuss. Chem. Soc.* **79** (1985) 55.
[13] DONALD A. M., VINEY C., WINDLE A. H., *Phil. Mag. B* **52** (1985) 925.
[14] HESSEL F., FINKELMANN H., *Polym. Bull.* **15** (1986) 349.
[15] EBERT M., HERRMANN-SCHONHERR O., WENDORFF J. H., RINGSDORF H., TSCHIRNER P., *Makromol. Chem. Rap. Commun* **9** (1988) 445.
[16] TOULOUSE G., *J. Phys. Lett.* **38** (1977) L-67.
[17] MALTHETE J., LIEBERT L., LEVELUT A. M., GALERNE Y., *C.R. Acad. Sci. Paris* **12** (1986).
[18] MIHAILOVIC M., OSWALD P., *J. Phys. France* **49** (1988) 1467.
[19] MACKLEY M. R., PINAUD F., SIEKMANN G., *Polymer* **22** (1981) 437.
[20] VINEY C., WINDLE A. H., *J. Mat. Sci.* **17** (1982) 2661.
[21] NOEL C., FRIEDRICH C., LAUPRETRE F., BILLARD J., BOSIO L., STRAZIELLE C., *Polymer* **25** (1984) 263.
[22] KLEMAN M., Liquid Crystallinity in Polymers A. Cifferi Ed. (VCM Publishers New York 1991).
[23] MEYER R. B., *Philos. Mag.* **27** (1973) 405.
[24] GRAZIANO D. J., MACKLEY M. R., *Mol. Cryst. Liq. Cryst.* **106** (1984) 73.
[25] WOOD B. A., THOMAS E. L., *Nature* (London) **324** (1986) 655.
[26] THOMAS E. L., WOOD B. A., *Faraday Discuss. Chem. Soc.* **79** (1985) 229.
[27] COGSWELL F. N., Recent Advances in LCP (Elsevier App. Sci. Publishers, 1985) chap. X.
[28] CALUNDANN G. W., JAFFE M., Proceedings of the Robert A. Welch conference on chemical research XXVI Synthetic Polymers, Houston (1982).
[29] HARTSHORNE N. H., STUART A., Crystals and the Polarising Microscope 4th Ed. Edward Arnold Ltd (London 1970).
[30] DE GENNES P. G., The Physics of Liquid Crystals (Clarendon Press Oxford GB, 1974).
[31] KLEMAN M., LIEBERT L., STRZELECKI L., *Polymer* **24** (1983) 295.
[32] MAZELET G., KLEMAN M., *Polymer* **27** (1986) 714.
[33] DE'NEVE T., NAVARD P., KLEMAN M., in preparation.